Chinese Journal of Natural Medicines

Combination of *AstragalusSalvia* and *OphiopogonDendrobium* herb pairs alleviates Sjgren's Syndrome *via* inhibiting the JAK1/STAT3 and PI3K/AKT pathways in NOD/Ltj mice

Peng Sun, Lili Zhu, Yang Yu, Sijing Hu, Mengyi Shan, Xuan Zhao, Xinchang Wang, Qiaoyan Zhang, Luping Qin

Citation: Peng Sun, Lili Zhu, Yang Yu, Sijing Hu, Mengyi Shan, Xuan Zhao, Xinchang Wang, Qiaoyan Zhang, Luping Qin, Combination of *AstragalusSalvia* and *OphiopogonDendrobium* herb pairs alleviates Sjgren's Syndrome *via* inhibiting the JAK1/STAT3 and PI3K/AKT pathways in NOD/Ltj mice, Chinese Journal of Natural Medicines, 2025, 23(6), 733−741. doi: 10.1016/S1875−5364(25)60892−2.

View online: https://doi.org/10.1016/S1875−5364(25)60892−2

Wechat

Chinese Journal of Natural Medicines 23 (2025) 733-741

Contents lists available at ScienceDirect

Chinese Journal of Natural Medicines

journal homepage: www.cjnmcpu.com/

Original article

Combination of *Astragalus–Salvia* and *Ophiopogon–Dendrobium* herb pairs alleviates Sjögren's Syndrome *via* inhibiting the JAK1/STAT3 and PI3K/AKT pathways in NOD/Ltj mice

Peng Sun[a,Δ], Lili Zhu[a,Δ], Yang Yu[a,Δ], Sijing Hu[a], Mengyi Shan[a], Xuan Zhao[a], Xinchang Wang[b,*], Qiaoyan Zhang[a,*], Luping Qin[a,*]

[a] *School of Pharmaceutical Sciences, Zhejiang Chinese Medical University, Hangzhou 310000, China*
[b] *Department of Rheumatology, the Second Affiliated Hospital, Zhejiang Chinese Medical University, Hangzhou 310000, China*

ARTICLE INFO

Article history:
Received 23 September 2024
Revised 2 November 2024
Accepted 5 December 2024
Available online 20 June 2025

Keywords:
Sjgren's syndrome
Astragalus-Salvia herb pair
Ophiopogon-Dendrobium herb pair
CXCL9 and CXCL10
JAK1/STAT3
PI3K/AKT

ABSTRACT

Sjögren's syndrome (SS) is an autoimmune disease characterized primarily by oral and periocular dryness. *Astragalus-Salvia* (AS) and *Ophiopogon-Dendrobium* (OD) represent two frequently utilized herb pairs in SS treatment. While the combination of AS-OD herb pairs demonstrates clinical efficacy in alleviating SS symptoms, its underlying mechanism remains unclear. This investigation sought to assess the therapeutic effects and elucidate the potential mechanisms of AS-OD in non-obese diabetic (NOD)/Ltj mice with SS. The study utilized NOD/Ltj mice as SS models, administering AS-OD treatment for 10 weeks at doses of 113.1, 226.2, and 339.3 mg·d^{-1}·20 g^{-1}. Results demonstrated that AS-OD improved SS symptoms, evidenced by enhanced salivary flow rate, decreased anti-SSA/Ro and anti-SSB/La antibody levels, increased swimming duration, and reduced lactate (LA) and blood urea nitrogen (BUN) levels in NOD/Ltj mice. AS-OD reduced lymphocyte infiltration, enhanced Aquaporin-5 (AQP5) expression in the submandibular gland, decreased inflammatory cytokine levels in the submandibular gland, and reduced the T helper type 17/regulatory T lymphocyte (Th17/Treg) cell ratio in the spleen. Transcriptomic and proteomic analyses indicated AS-OD's involvement in regulating phosphatidylinositol-3-kinase/protein kinase B (PI3K/AKT) and Janus kinase 3/signal transducer and activator of transcription 3 (JAK1/STAT3) pathways, with inhibitory effects validated in both NOD/Ltj mice submandibular gland and A-253 cells. Furthermore, AS-OD enhanced cell viability and reduced A-253 cell apoptosis through the PI3K/AKT pathway. In A-253 cells, AS-OD reduced inflammatory cytokine levels, CXC chemokine ligand 9/10 (CXCL9/10), and T-cell chemotaxis by inhibiting the JAK1/STAT3 pathway. AS-OD mitigates SS by suppressing inflammation and immune responses through the PI3K/AKT and JAK1/STAT3 pathways.

1. Introduction

Sjögren's syndrome (SS) is one of the most prevalent inflammatory autoimmune diseases, characterized by oral and ocular dryness with systemic complications including purpura, kidney damage, lung disease, chronic hepatitis, and neurologic disease, with an overall incidence of approximately 0.5% [1]. The etiology of SS relates to genetics, hormones, environmental factors, and viral infections, which result in substantial lymphocyte infiltration into the exocrine glands, ultimately triggering chronic inflammation and secretory dysfunction [2]. Current therapy for SS primarily includes symptomatic relief for sicca syndrome and immunosuppressive interventions for systemic symptoms. Xerostomia treatment typically involves oral muscarinic agonists and artificial saliva, while xerophthalmia is addressed with artificial tear drops and topical non-steroidal anti-inflammatory drugs. Systemic symptoms of SS are generally managed with hydroxychloroquine, oral glucocorticoids, and synthetic immunosuppressants [3]. However, these oral medications present limitations and adverse effects, and there remains a lack of reliable therapy to alleviate SS symptoms. For instance, prolonged use of oral muscarinic agonists may induce sweating, flushing, headaches, and nausea, while extended use of artificial saliva can promote dental caries and oral infections [4]. Systemic immunosuppressive therapy increases infection risk, and certain drugs produce adverse effects, including dizziness, vomiting, gastrointestinal disorders, hypertension, or kidney disease [5]. Therefore, developing safe, effective, and durable therapeutic strategies for SS remains imperative.

Traditional Chinese herbal medicines demonstrate a well-established history and have garnered attention as promising complementary and alternative therapies for treating rheumatism and immunity diseases, owing to their affordability, gentle

* Corresponding author.
E-mail addresses: ossani@126.com (X. Wang); zqy1965@163.com (Q. Zhang); lpqin@zcmu.edu.cn (L. Qin)
Δ These authors contributed equally to this work.

https://doi.org/10.1016/S1875-5364(25)60892-2

nature, long-lasting effects, and low toxicities [6]. According to the theory of Traditional Chinese Medicine (TCM), SS is attributed to insufficiency of "*Qi*" and "*Yin*", as well as pathological dryness and blood stasis. Thus, SS treatment prioritizes the principle of "benefiting *Qi*, nourishing *Yin*, moisturizing dryness, and dispelling stasis". A meta-analysis encompassing 2137 cases indicated that Chinese herbal medicines demonstrated significantly higher efficacy and lower adverse effect rates in SS clinical treatment compared to chemically synthesized medicines [7]. Given that *Astragalus membranaceus* Fisch. ex Bunge (*Huangqi* in Chinese) benefits *Qi*, and *Salvia miltiorrhiza* Bunge (*Danshen* in Chinese) dispels stasis, the herb pair of *Astragalus-Salvia* (AS) enhances the therapeutic effects of "benefiting Qi by Huangqi and dispelling stasis by Danshen" [8]. *Ophiopogon japonicus* (Thunb.) Ker Gawl. (*Maidong* in Chinese) and *Dendrobium officinale* Kimura et Migo (*Tiepishihu* in Chinese) excel in "nourishing *Yin* and moisturizing dryness", while the herb pair of *Ophiopogon-Dendrobium* (OD) demonstrates complementary enhancement of therapeutic effects [9]. Both herb pairs represent frequently used clinical treatments for SS and appear in numerous classic formulas. The AS-OD herb pairs combination better aligns with TCM treatment principles for SS than using individual herb pairs and has served as an in-hospital preparation across multiple hospitals. AS-OD demonstrates satisfactory therapeutic efficacy in SS treatment by increasing Aquaporin-5 (AQP5) and muscarinic type 3 receptor expression to enhance salivary flow in NOD mice and by alleviating oral dryness, pain, and fatigue in SS patients [10, 11]. However, the precise action mechanisms of AS-OD on SS remain unclear.

As transcriptomics and proteomics technology has emerged as a vital approach for exploring complex mechanisms of TCM, this study employs these technologies to unravel the underlying mechanisms by which AS-OD mitigates SS, and further validates the results by analyzing the interaction pathways of integrated omics. This study demonstrates that AS-OD promotes salivary secretion, alleviates fatigue, regulates the T helper type 17/regulatory T lymphocyte (Th17/Treg) ratio, suppresses CXC chemokine ligand 9/10 (CXCL9/10) production, and attenuates inflammation *via* the Janus kinase 3/signal transducer and activator of transcription 3 (JAK1/STAT3) and phosphatidylinositol-3-kinase/protein kinase B (PI3K/AKT) pathway. These findings provide a scientific basis for AS-OD clinical application.

2. Materials and methods

2.1. Materials

The dried roots of *Astragalus membranaceus* Fisch. ex Bunge (Astragali radix, LOT20210602), dried roots and rhizomes of *Salvia miltiorrhiza* Bunge (Salviae miltiorrhizae radix et rhizome, LOT20210301), dried roots of *Ophiopogon japonicus* (Thunb.) Ker Gawl. (Ophiopogonis radix, LOT20210701) and caulis of *Dendrobium officinale* Kimura et Migo (Dendrobii officinalis caulis, LOT20210601) were obtained from Zhejiang Chinese Medical University Chinese Herbal Pieces Co., Ltd. (Hangzhou, China). Professor Lu-Ping Qin authenticated the herbal materials through pharmacognostic analysis. Each specimen received a unique voucher number and was systematically cataloged in the research group's herbarium for reference purposes.

2.2. Preparation of AS-OD and analysis of chemical compounds

The standard decoction was prepared by combining Astragali radix, Salviae miltiorrhizae radix et rhizome, Dendrobii officinalis caulis, and Ophiopogonis radix in a 4 : 5 : 10 : 10 ratio. The herbs were soaked in distilled water (10-fold volume) for 30 min, boiled for 2 h, and filtered through gauze. This extraction process was performed three times. The combined filtrates were concentrated *via* rotary evaporation to achieve a crude drug concentration of 1000 mg·mL^{-1}. UPLC-MS/MS analysis was employed to characterize the chemical components of the aqueous decoction (detailed methodology available in Supplementary Material).

2.3. Animals

Female specific pathogen-free (SPF) Institute of Cancer Research (ICR) mice (23 ± 5 g) and female SPF non-obese diabetic (NOD)/Ltj mice (SS model mice, 20 ± 3 g) aged 5–6 weeks were acquired from Gempharmatech Co., Ltd. in Nanjing, China. The animals were maintained under controlled conditions at 24 ± 1 °C with 60 ± 5% humidity. The study adhered to US guidelines for laboratory animal use and care, with approval from the Committee on the Ethics of Animal Experiments of Zhejiang Chinese Medical University (Ethics permit No. 12603). The NOD/Ltj mice were divided into five groups: model group, TOF group (tofacitinib, 2.6 mg·d^{-1}·20 g^{-1}), low-dose AS-OD group (113.1 mg·d^{-1}·20 g^{-1}), medium-dose AS-OD group (226.2 mg·d^{-1}·20 g^{-1}) and high-dose AS-OD group (339.3 mg·d^{-1}·20 g^{-1}). Oral gavage administration commenced at week 8 and continued for 10 weeks.

2.4. Salivary flow measurement

Salivary flow rates were assessed in mice at 6, 10, 14, and 18 weeks of age. Following anesthesia, mice received pilocarpine injections (2.5 μg·25 g^{-1}) to stimulate salivary secretion. Saliva was collected over a 10-minute period and quantified volumetrically.

2.5. Fatigue test

Fatigue assessment utilized a forced swimming protocol. Individual mice were placed in a swimming pool (60 cm × 50 cm × 40 cm) containing water at 26 ± 1 °C to a depth of 30 cm. A lead strip weighing 10% of each mouse's body weight was attached to the tail base. Swimming time was recorded until exhaustion, defined as failure to surface within 10 seconds. Post-swimming blood samples were analyzed for lactate (LA) and blood urea nitrogen (BUN) levels.

2.6. Histological assessment

Submandibular glands tissues underwent hematoxylin-eosin (H&E) staining. Lesion scoring was based on lymphocyte foci count per 4 mm^2 in the submandibular glands (lesions were defined as ≥ 50 lymphocytes).

2.7. Immunohistochemistry (IHC) of the submandibular glands

Submandibular gland sections underwent dewaxing under high pressure and rehydration, followed by citrate buffer treatment and natural cooling. After blocking, sections were incubated with primary antibody overnight at 4 °C, followed by secondary antibody incubation. The sections were then dried and scanned, with subsequent image analysis performed using ImageJ.

2.8. Determination of anti-SSA/Ro and anti-SSB/La antibodies and cytokines

Serum levels of mouse anti-SSA/Ro and anti-SSB/La antibodies and cytokines were measured using ELISA kits (anti-SSA/Ro antibodies, anti-SSB/La antibodies, Alpha Diagnostic International, USA); tumor necrosis factor-α (TNF-α), interferon-γ (IFN-γ), interleukin 1β (IL-1β), IL-6, IL-18, CXCL9, CXCL10, Liankebio, China).

2.9. Transcriptomic analysis

Five mice were randomly selected from each of the control, model, and high-dose AS-OD treatment groups. Ribonucleic acid (RNA) was extracted from the submandibular gland using TRIzol (Invitrogen, USA) for sequencing and transcriptomic analysis. Detailed procedures are presented in Supplementary Materials. Data processing was performed using Cutadapt version 1.9, which eliminated reads containing adapter, poly A and poly G, unknown nucleotides (N), and low-quality bases. Differentially expressed genes (DEGs) were identified using an FDR threshold below 0.05 and a minimum absolute fold change of 2. The data have been deposited to the NCBI GEO Datasets (ID: GSE247662).

2.10. Proteomic analysis

The tissue samples for proteomics analysis were from the same batch used for transcriptomics. Equal quantities of protein were extracted from each sample, and trypsin was added at a protein-to-enzyme ratio of 50 : 1. The resulting peptides underwent desalting using a solid-phase extraction column (Waters, USA), followed by vacuum-drying and dissolution in TEAB. Peptide labeling was performed according to the TMT pro™ 16plex Label Reagent guidelines (Thermo Scientific, USA). Mass spectrometry conditions are detailed in the supplementary materials. Protein identification and quantitative analysis were conducted using MaxQuant software, version 2.1.4.0. Differentially expressed proteins (DEPs) were identified using an absolute fold change of ≥ 1.2 and an FDR threshold below 0.05. The mass spectrometry proteomics data have been deposited to the ProteomeXchange Consortium *via* the iProX partner repository (dataset identifier: PXD051120).

2.11. Western blot

The processed proteins underwent electrophoresis and membrane transfer operations. The membranes were treated with specific primary antibodies against β-actin, PI3K, AKT, JAK1, STAT3, phosphorylated (p)-PI3K, p-AKT, p-JAK, p-STAT3 (Cell Signaling Technology, USA), followed by corresponding secondary antibodies. Protein detection was performed using an electrochemiluminescence reagent, and membrane imaging was conducted using a chemiluminescent imager.

2.12. Preparation of AS-OD-containing serum

Female ICR mice weighing 23 ± 5 g were randomly divided into four groups: control, low-dose AS-OD, medium-dose AS-OD, and high-dose AS-OD, and received the relevant drug *via* gavage for seven consecutive days. The AS-OD dosage remained consistent with previous administrations. Blood samples were subsequently collected and centrifuged to obtain serum, which was inactivated in a water bath at 60 °C.

2.13. Cell treatment

A-253 cells derived from the human submandibular gland were obtained from KeyGEN BioTECH (Jiangsu, China), while Jurkat T cells were obtained from iCELL (Shanghai, China). Both cell lines were cultured in RPMI-1640 medium supplemented with 10% fetal bovine serum. For experimental grouping, A-253 cells were divided as follows: control group (untreated cells), model group (cells stimulated with 20 $ng \cdot mL^{-1}$ TNF-α and IFN-γ for 12 h), positive control group (cells treated with 10 $\mu mol \cdot L^{-1}$ of either the JAK1 inhibitor tofacitinib or the PI3K inhibitor LY294002 after stimulation for 12 h), AS-OD-containing serum groups (cells treated with 10% (*V/V*) low, medium, or high concentrations of AS-OD-containing serum after stimulation for 12 h), and H + PI3Ka group (cells treated with a high concentration of AS-OD-containing serum and 20 $\mu mol \cdot L^{-1}$ of the PI3K agonist 4-methylbenzylidene camphor after stimulation for 12 h). An equal volume of blank serum, derived from the same source but lacking AS-OD, was added to the groups not receiving AS-OD-containing serum.

2.14. T-cell migration assay

Cell migration assay was conducted to evaluate the directional migration of Jurkat T cells induced by the supernatant of treated A-253 cells. The supernatant containing 600 μL treated cells was placed in the bottom chambers, while 5×10^5 Jurkat T cells in 200 μL basic medium were seeded in the migration chamber and incubated for 24 h. T cell migration to the bottom chambers was quantified using CCK-8 assay.

2.15. Small interfering RNA (siRNA) transfection

A siRNA-mediated knockdown approach was employed to specifically silence JAK1 gene expression in A-253 cells. The silencing siRNA targeting JAK1 was designed and constructed by riboFECT CP Transfection Kit (RIBOBIO, China), comprising three siRNAs, with the most effective one selected through preliminary experiments. Transfection complexes were prepared using the riboFECT CP Transfection Kit (RIBOBIO, China). A-253 cells in the NC + MOD group received blank transfection complexes for model group cells, while cells in the siJAK1 group received JAK1-siRNA transfection complexes. A-253 cells in the siJAK1 + H or siJAK1 + TOF groups were incubated with a high dose of AS-OD-containing serum or TOF for 12h following JAK1 silencing treatment, respectively, to verify AS-OD's action through the JAK1 pathway.

2.16. Molecular docking and molecular dynamics simulations

A total of 131 compounds identified in AS-OD underwent energy minimization while maintaining specified chiralities. The protein underwent pretreatment for bond order assignment, hydrogen addition, and H-bond assignment optimization. Molecular docking was conducted using the AutoDock Vina module of PyMOL. Subsequently, the top 30 compounds were selected for molecular dynamics simulations. The System Builder module in Maestro employed TIP3P($10 \times 10 \times 10$ $Å^3$) as a predefined solvent model to construct the ligand-receptor complex system in the OPLS3 force field. The system was heated to 300 K in the NPT ensemble, with the final pressure maintained at 1.01325 bars. Dynamics simulations were performed for 10 ns in a protein-receptor complex system with trajectories recorded at 10 ps intervals.

2.17. Cellular thermal shift assay (CETSA)

A-253 cells were treated with the compounds for 2 h. The cells were then digested with trypsin, dispensed into six PCR tubes, heated to the indicated temperatures (45, 49, 53, 57, 61, 65 °C for JAK1; 37, 41, 45, 49, 53, 57 °C for PI3K) for 3 min, and immediately snap frozen in liquid nitrogen. The samples underwent three freeze-thaw cycles and centrifugation at 12 000 g for 20 min. The supernatant was collected for Western blot analysis.

2.18. Statistical analysis

The data are presented as the mean ± S.D. Statistical analysis was performed using GraphPad Prism (California, USA) with a one-way ANOVA followed by Dunnett's multiple comparisons

test. A value of $P < 0.05$ was considered statistically significant.

3. Results

3.1. Characterization of the chemical compounds in AS-OD

Analysis of AS-OD's chemical composition revealed 131 compounds, including 31 compounds from Dendrobii officinalis caulis, 27 from Ophiopogonis radix, 29 from Astragali radix, and 46 from Salviae miltiorrhizae radix et rhizoma. The identified compounds were classified into four major categories: 32 flavonoids, 23 saponins, 18 naphthoquinones, and 12 terpenoids. Their chemical structures and related information are presented in Figure S1 and Table S1.

3.2. AS-OD alleviates SS symptoms in NOD/Ltj mice

As illustrated in Fig. 1A, the salivary flow rate decreased significantly in model group mice during experiments from 6 to 18 weeks compared to the control group. AS-OD treatment significantly enhanced the salivary flow rate at 14 and 18 weeks in NOD/Ltj mice. Furthermore, serum levels of anti-SSA/Ro antibody and anti-SSB/La antibody were significantly elevated in NOD/Ltj mice, and administration of TOF and AS-OD significantly reduced these antibody levels (Figs. 1B, 1C). These findings demonstrate AS-OD's effectiveness in attenuating SS symptoms.

Histopathological analysis was conducted using HE staining and IHC for AQP5 protein in submandibular gland tissues. The H&E staining revealed increased lymphocytic infiltration and foci, with elevated pathology scores in the submandibular gland of NOD/Ltj mice compared to the control group. Treatment with TOF and AS-OD effectively reversed these pathological alterations in the submandibular glands (Figs. 1D, 1E). Furthermore, immunohistochemical analysis demonstrated significantly decreased AQP5 expression in the submandibular glands compared to the control group, while AS-OD treatment enhanced AQP5 expression (Figs. 1F, 1G), suggesting that AS-OD ameliorated both lymphocytic infiltration and AQP5 expression in the submandibular gland of NOD/Ltj mice.

As illustrated in Fig. 1H, NOD/Ltj mice exhibited significantly decreased forced swimming duration, which AS-OD treatment substantially extended. Additionally, NOD/Ltj mice showed elevated BUN levels, while AS-OD treatment significantly reduced both LA and BUN levels (Figs. 1I, 1J, indicating that AS-OD effectively alleviated SS-induced fatigue in NOD/Ltj mice.

3.3. AS-OD modulates inflammation and immune responses in NOD/Ltj mice and A-253 cells stimulated with TNF-α and IFN-γ

Given that SS patients typically present with elevated cytokine levels, inflammatory cytokines in the submandibular gland were analyzed. The model group exhibited significantly increased levels of TNF-α, IFN-γ, IL-1β, IL-6, and IL-18 compared to the control group, while AS-OD treatment markedly reduced these cytokine levels (Fig. 2A). Moreover, AS-OD treatment decreased IL-1β and IL-6 levels in TNF-α and IFN-γ-stimulated A-253 cells (Fig. 2B). Chemokines, particularly CXCL9/10, are crucial in SS immunoreaction, with CXC chemokine receptor 3 (CXCR3) serving as a CXCL9/10 receptor and marker for immune cell infiltration [12]. Results demonstrated significantly elevated CXCL9/10 levels in submandibular gland tissue compared to the control group, which AS-OD treatment significantly reduced (Fig. 2D), indicating AS-OD's inhibitory effect on CXCL9/10 production. Furthermore, TNF-α and IFN-γ stimulation induced a significant elevation of CXCL9/10 levels and T cell chemotaxis in A-253 cells, which AS-OD treatment diminished (Fig. 2). AS-OD's effects on T cell differentiation were evaluated by analyzing Th17

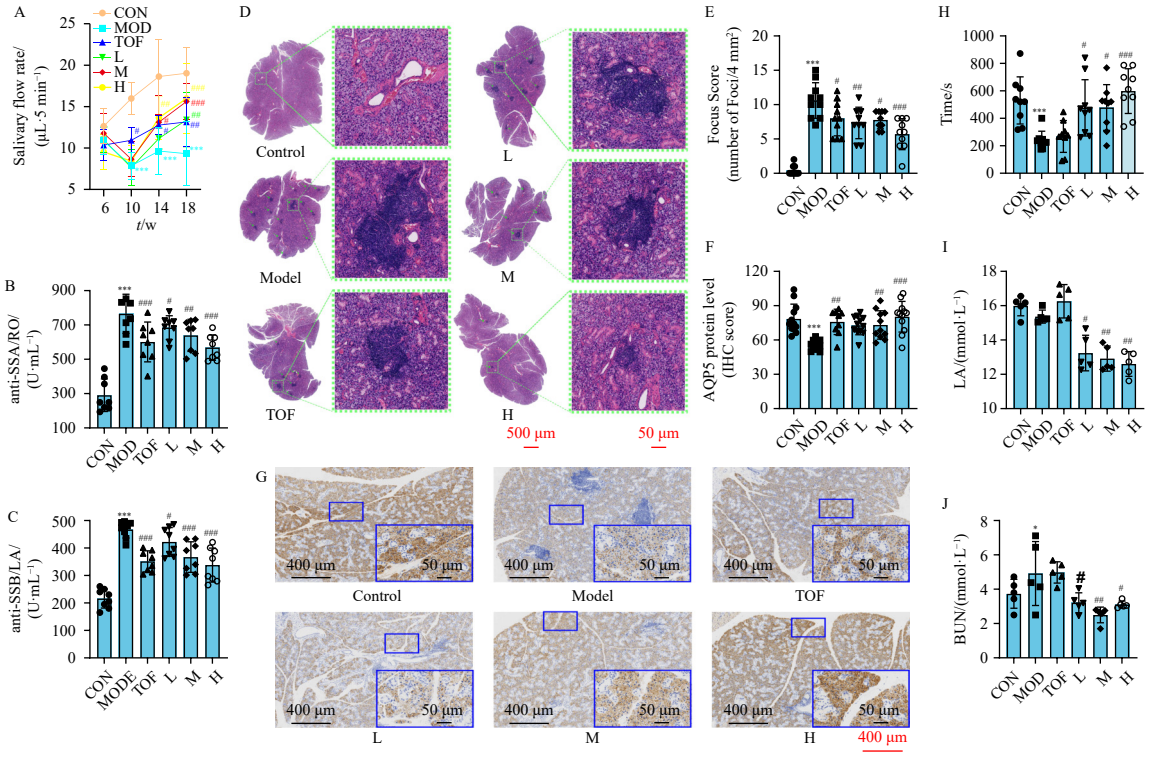

Fig. 1 AS-OD alleviates symptoms of SS in NOD/Ltj mice. (A) The salivary flow rate of mice at 6, 10, 14 and 18 weeks ($n = 10$); (B–C) Levels of anti-SSA/Ro and anti-SSB/LA ($n = 10$); (D) H&E staining of submandibular gland tissue sections, enlarged image shows lymphocytic infiltration, the scale bars represent 500 μm and 50 μm ($n = 10$); (E) The focus score of the submandibular gland in H&E staining ($n = 10$); (F) IHC score of AQP5 protein level ($n = 10$); (G) Immunohistochemical staining of AQP5 in the submandibular gland, and the scale bars represent 400 μm (overview) and 50 μm (inset); (H–J) The forced swimming time, LA and BUN ($n = 10$). (Mean ± SD, $^{*}P < 0.05$, $^{**}P < 0.01$, $^{***}P < 0.001$, *vs* control group; $^{\#}P < 0.05$, $^{\#\#}P < 0.01$, $^{\#\#\#}P < 0.001$ *vs* model group)

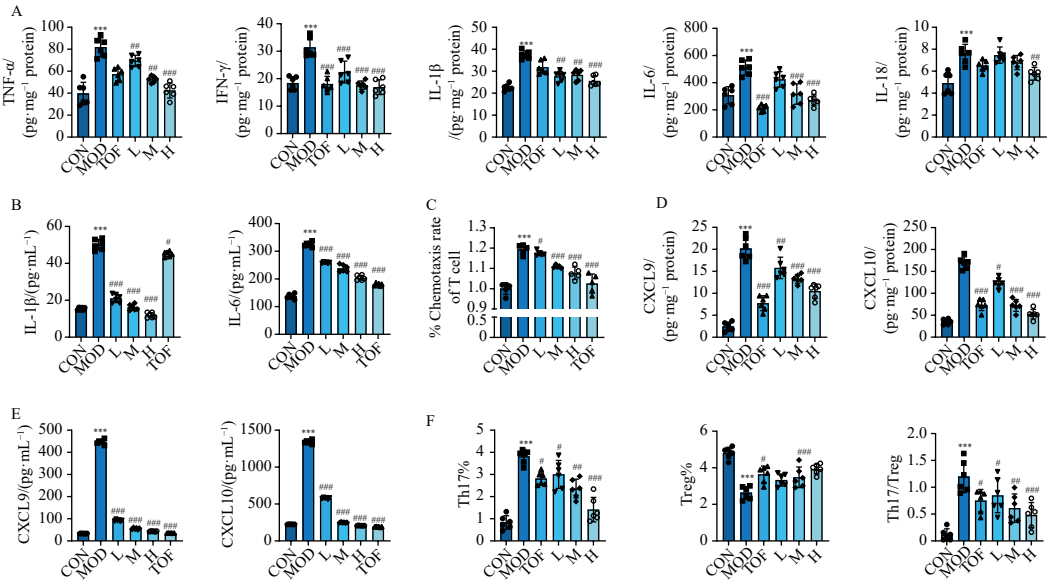

Fig. 2 AS-OD inhibits the levels of inflammatory cytokines and regulates Th17/Treg cells. (A) Levels of TNF-α, IFN-γ, IL-1β, IL-6, and IL-18 in the submandibular gland (n = 6); (B) Levels of IL-1β and IL-6 in A-253 cells (n = 6); (C) Chemotaxis of Jurkat T cells (n = 6); (D) Levels of CXCL9 and CXCL10 in the submandibular gland (n = 6); (E) Levels of CXCL9 and CXCL10 in A-253 cells (n = 6); (F) Proportion of Th17/Treg cell in the spleen (n = 6). (Mean ± S.D, $^{*}P < 0.05$, $^{**}P < 0.01$, $^{***}P < 0.001$ *vs* control group; $^{\#}P < 0.05$, $^{\#\#}P < 0.01$, $^{\#\#\#}P < 0.001$ *vs* model group).

cells (cluster of differentiation 4 $(CD4)^{+}$ $IL\text{-}17^{+}$) and Treg cells ($CD4^{+}FoxP3^{+}$) proportions in NOD/Ltj mice spleen tissue. NOD/Ltj mice showed significantly increased Th17 cells and decreased Treg cells compared to controls (Figs. 2F, S2). AS-OD treatment effectively reduced Th17 cell percentage while increasing Treg cell percentage, resulting in a significant reduction of the Th17/Treg cell ratio in NOD/Ltj mice spleen tissue.

3.4. AS-OD treatment alters the transcriptomics and proteomics profile of NOD/Ltj mice

Transcriptomic and proteomic analyses serve as valuable tools for elucidating drug mechanisms. To investigate the regulatory mechanism of AS-OD on SS, DEGs and proteins (DEPs) were analyzed in the submandibular gland tissue of NOD/Ltj mice. Transcriptomic analysis revealed 543 up-regulated and 478 down-regulated DEGs following AS-OD treatment (Fig. S3A–F). Gene Ontology (GO) and Kyoto Encyclopedia of Genes and Genomes (KEGG) analyses of these DEGs indicated that AS-OD's pharmacological effects were linked to CXCR3 chemokine receptor binding, amylase activity, immune response, and chemokine-mediated signaling pathways. KEGG pathway enrichment analysis further demonstrated associations with chemokines, cytokines, and T cells.

The proteomic analysis identified 163 up-regulated and 122 down-regulated DEPs in the submandibular gland tissue of AS-OD-treated NOD/Ltj mice (Figs. S3G–L). GO analysis revealed that these DEPs are primarily related to cytoplasm, nucleus, protein binding, and immune system processes. The KEGG enrichment pathways predominantly involved inflammation, Th17 cell-associated processes, and chemokine pathways.

The pathway interactions identified through transcriptomic and proteomic KEGG enrichment analysis are illustrated in Fig. 3A, highlighting the predominant roles of PI3K/AKT signaling pathway, JAK/STAT signaling pathway, chemokine signaling pathway, cytokine-cytokine receptor interaction, T cell receptor signaling pathway, and Th17 cell differentiation. A Venn diagram analysis of transcriptomic DEGs and proteomic DEPs revealed 11 overlapping DEGs/DEPs (Fig. 3B): Creb1, Gnmt, Rara, Kctd14, Lpin1, Nell1, Pik3cg, JAK1, Siglec1, St6galnac1, and STAT3. PPI analysis of these DEGs/DEPs (Fig. 3C) demonstrated that STAT3 interacts with Creb1, Rara, Pik3cg, and JAK1. Heatmap analysis of DEPs/DEGs revealed significant positive correlations among Pik3cg, JAK1, and STAT3, while showing a significant negative correlation with St6galnac1 (Fig. 3D). Furthermore, Rara, Pik3cg, JAK1, Siglec1, and STAT3 exhibited elevated levels in the model group and decreased levels in the AS-OD group, whereas Gnmt showed the opposite pattern. These trends remained consistent at both transcriptome and proteome levels (Figs. 3E, 3F). Notably, Pik3cg and JAK1 demonstrated significant variations in both transcript and protein levels. Given that Pik3cg is associated with the PI3K/AKT pathway, and JAK1 and STAT3 are components of the JAK/STAT pathway, these pathways were identified as potential mechanisms for AS-OD action, warranting further validation in subsequent experiments.

3.5. AS-OD suppresses apoptosis of submandibular gland cells by inhibiting the PI3K/AKT pathway

The PI3K/AKT pathway serves a crucial function in regulating cell proliferation, growth, apoptosis, and autophagy [13]. Transcriptomic and proteomic analyses demonstrated that AS-OD regulated the PI3K/AKT pathway in the submandibular gland of NOD/Ltj mice. Additional investigation revealed significantly elevated phosphorylation levels of PI3K and AKT in the submandibular gland of NOD/Ltj mice compared to control mice. Western blot and HIC staining analyses demonstrated that AS-OD treatment inhibited PI3K/AKT pathway activation (Figs. 4A–4C). AS-OD significantly reduced PI3K and AKT phosphorylation in stimulated A-253 cells (Fig. 4D) while substantially enhancing cell viability and reducing apoptosis (Figs. 4E–4G). The introduction of PI3K agonist diminished AS-OD's effects on viability and apoptosis in A-253 cells stimulated with TNF-α and IFN-γ, suggesting that AS-OD mitigates decreased cell viability and increased apoptosis through PI3K/AKT pathway inhibition.

3.6. AS-OD reduces the levels of inflammatory cytokines and CXCL9/10 by inhibiting JAK1/STAT3 pathway in NOD/Ltj mice and A-253 cells stimulated with TNF-α and IFN-γ

Analysis of protein phosphorylation expressions of JAK1/STAT3 through Western Blot and IHC staining revealed signific-

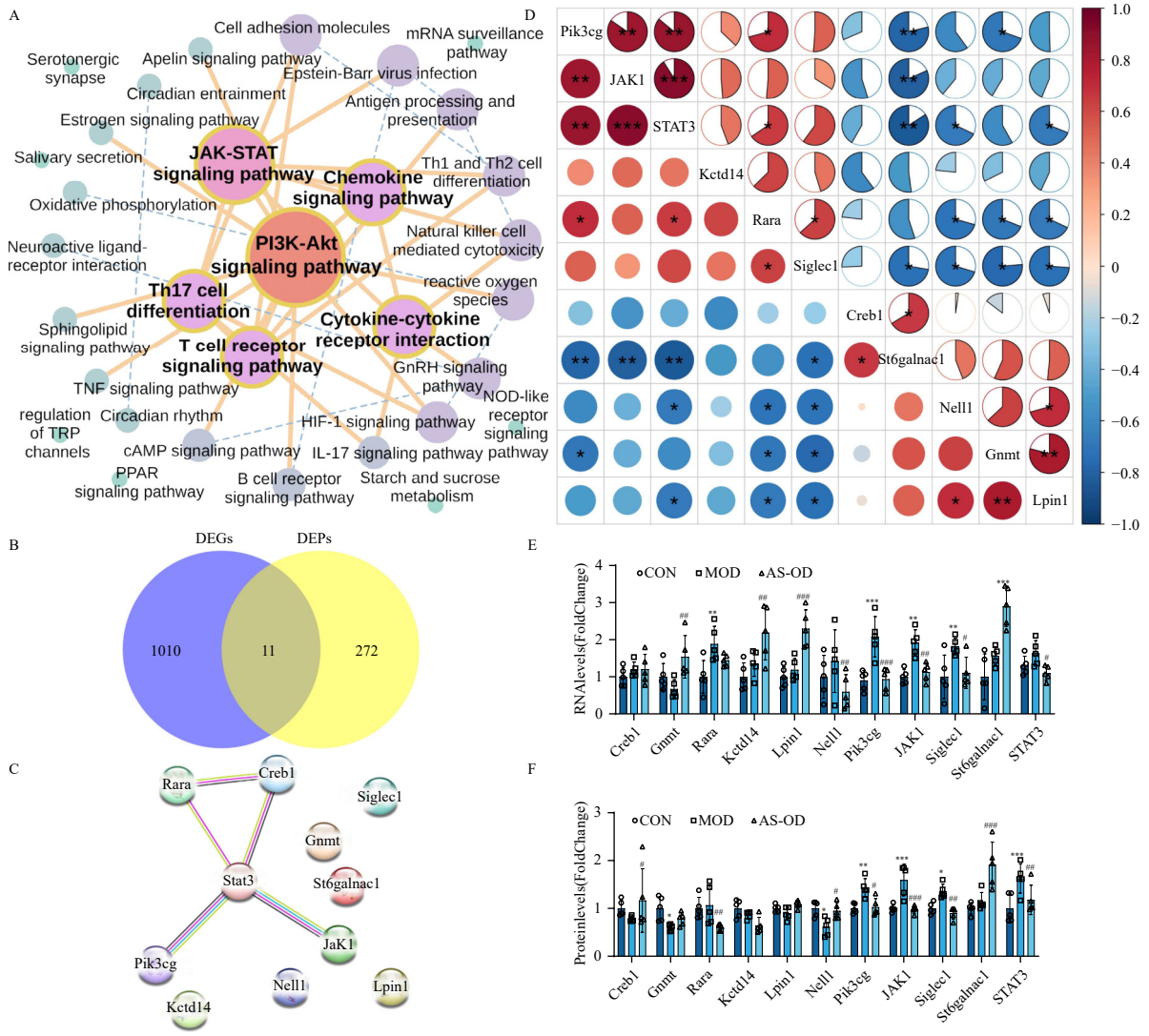

Fig. 3 Joint analysis of transcriptomics and proteomics. (A) Network Diagram of Multi-omics Enrichment Pathway Interactions; (B) Venn Diagram of DEGs and DEPs; (C) PPI network of 11 DEGs/DEPs; (D) Heatmap of 11 DEGs/DEPs; (E) RNA levels of DEGs (n = 5); (F) Protein levels of DEPs (n = 5). (Mean ± SD, $^{*}P < 0.05$, $^{**}P < 0.01$, $^{***}P < 0.001$ *vs* control group; $^{\#}P < 0.05$, $^{\#\#}P < 0.01$, $^{\#\#\#}P < 0.001$ *vs* model group)

antly elevated JAK1 and STAT3 phosphorylation levels in the submandibular gland tissue of NOD/Ltj mice compared to the control group. AS-OD treatment significantly reduced the phosphorylation of JAK1 and STAT3 (Figs. 5A–5C). Furthermore, TNF-α and IFN-γ stimulation induced significant elevation of JAK1/STAT3 phosphorylation in A-253 cells, while AS-OD treatment decreased phosphorylation of JAK1 and STAT3 in these stimulated cells (Fig. 5D). The JAK1/STAT3 pathway commonly regulates inflammatory cytokines in SS [14]. JAK1 gene silencing decreased IL-6 and CXCL9/10 production in stimulated A-253 cells and diminished AS-OD's inhibitory effects on IL-6 and CXCL9/10 production, indicating that AS-OD reduced the production of IL-6 and CXCL9/10 through JAK1/STAT3 pathway suppression (Figs. 5E–5G).

3.7. Prediction and validation of active chemical compounds in AS-OD based on JAK1 and PI3K

To elucidate the active components in AS-OD, molecular docking, molecular dynamics simulations, CETSA, and validation in A-253 cells were conducted. The molecular docking diagram of JAK1 in Fig. 6A demonstrates that methylophiopogonanone B, miltirone I, neocryptotanshinone, cryptotanshinone, and tanshinone I exhibit favorable binding properties with JAK1 proteins, primarily through intermolecular forces and hydrogen bonding. Molecular dynamics simulations analysis revealed that the root-mean-square deviation (RMSD) value of the ligand-JAK1 complexes remained within 4 Å, indicating a reasonably stable conformation of JAK1 molecular docking (Fig. 6B). Specific virtual screening scores are presented in Table S2. Based on the predicted results, the three most promising compounds were selected for CETSA and cellular experiments to verify direct protein binding and efficacy. As illustrated in Fig. 6C, cryptotanshinone, tanshinone I, and neocryptotanshinone significantly inhibited high-temperature-induced degradation of JAK1 proteins at 53, 57, 61, and 65 °C, enhancing protein thermal stability compared to the DMSO group, suggesting direct binding to JAK1. Additionally, all three compounds significantly reduced CXCL9/10 levels in TNF-α and IFN-γ-stimulated A-253 cells (Fig. 6D).

The molecular docking diagram of PI3K (Fig. 6E) demonstrated that Van der Waals forces and hydrogen bonds mediate the affinities between PI3K and rhamnocitrin, rutin, diosmetin7-*O*-β-*D*-glucopyranoside, naringenin, and 2,4,7-Trihydroxy-9,10-dihydrophenanthrene. Molecular dynamics simulations analysis demonstrated RMSD values below 4 Å, supporting the stability of PI3K molecular docking conformations in the ligand-receptor complexes (Fig. 6F). As shown in Fig. 6G, rutin significantly enhanced PI3K protein expression at 45, 49, 53, and 57 °C com-

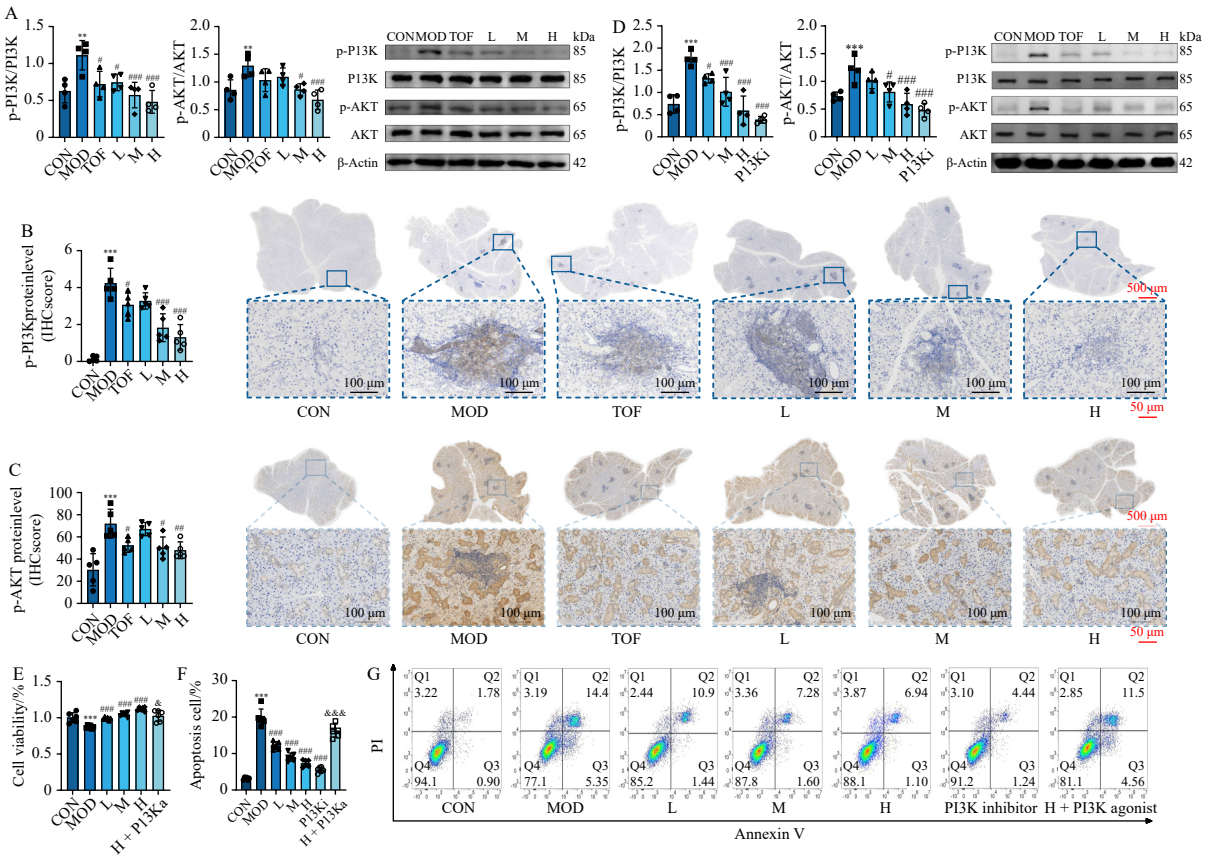

Fig. 4 AS-OD reduces apoptosis of submandibular gland cells *via* inhibiting the PI3K/AKT signaling pathway. (A) Western blot and quantitative analysis on PI3K/AKT pathway in the submandibular glands (n = 4); (B–C) Immunohistochemical staining of p-PI3K and p-AKT in the submandibular glands, and the scale bars represent 500 μm and 50 μm (n = 5); (D)Western blot and quantitative analysis on PI3K/AKT pathway in A-253 cells (n = 4); (E) Viability of A-253 cells (n = 5); (F–G)The apoptosis ratio of A-253 cells (n = 5). (Mean ± SD, $^{**}P < 0.01$, $^{***}P < 0.001$ *vs* control group; $^{\#}P < 0.05$, $^{\#\#}P < 0.01$, $^{\#\#\#}P < 0.001$ *vs* model group; $^{\&\&\&}P < 0.001$ *vs* H group)

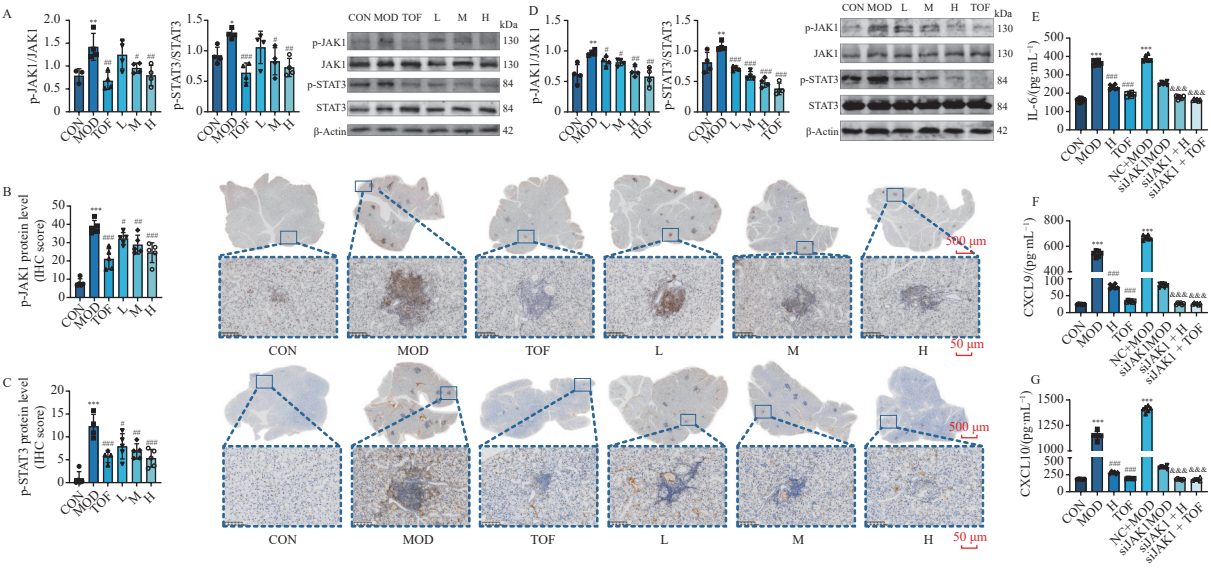

Fig. 5 AS-OD suppresses JAK1/STAT3 signaling pathway to inhibit the production of IL-6, CXCL9 and CXCL10. (A) Western blot and quantitative analysis on JAK1/STAT3 pathway in the submandibular glands (n = 4); (B–C) Immunohistochemical staining of p-JAK1 and p-STAT3 in the submandibular glands, and the scale bars represent 500 μm and 50μm (n = 5); (D) Western blot and quantitative analysis on JAK1/STAT3 pathway in A-253 cells (n = 4); (E–G) Levels of IL-6, CXCL9 and CXCL10 after si-JAK1 transfection in A-253 cells (n = 5). (Mean ± SD, $^{**}P < 0.01$, $^{***}P < 0.001$ *vs* control group; $^{\#}P < 0.05$, $^{\#\#}P < 0.01$, $^{\#\#\#}P < 0.001$ *vs* model group; $^{\&\&\&}P < 0.001$ *vs* JAK1-siRNA model group)

pared to the DMSO group, indicating that its direct binding to PI3K increased PI3K thermal stability. Among the three compounds tested, rutin demonstrated significant enhancement of viability and inhibition of apoptosis in TNF-α and IFN-γ-stimulated A-253 cells (Fig. 6H).

4. Discussion

SS is a multisystem autoimmune disease characterized by salivary and lacrimal gland hypoplasia. The classification criteria established by the American College of Rheumatology/European

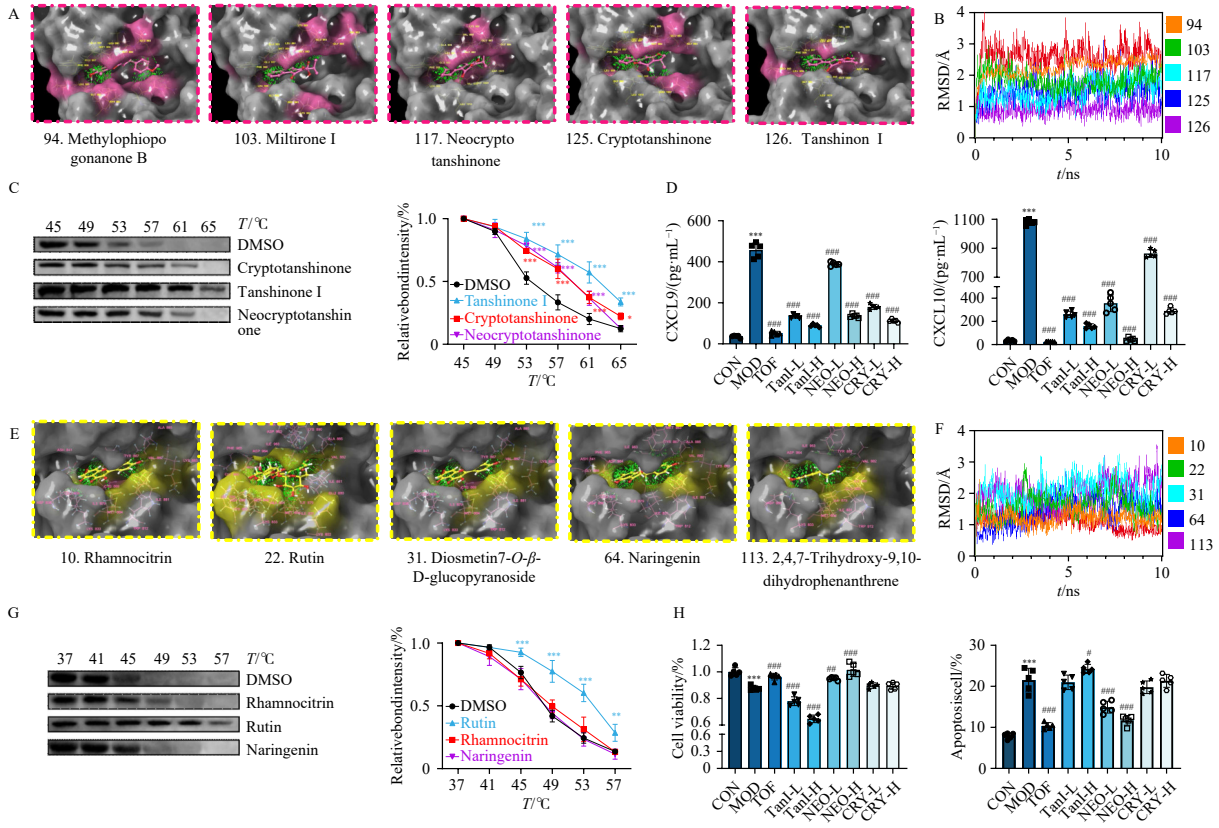

Fig. 6 The molecular docking, CETSA, and validation of compounds. (A) The docking results of the compounds in complex of JAK1; (B) The RMSD plots of compound-JAK1 complex in molecular dynamics simulations; (C) CETSA evaluation of binding between compounds and JAK1 (45–65 °C for JAK1, interval temperature: 4 °C, n = 3); (D) Levels of CXCL9 and CXCL10 in A-253 cells (n = 5); (E) The docking results of the compounds in complex of PI3K; (F) The RMSD plots of compound-PI3K complex in molecular dynamics simulations; (G) CETSA evaluation of binding between compounds and PI3K (37–57 °C for PI3K, interval temperature: 4 °C, n = 3); (H) The viability and apoptosis ratio of A-253 cells (n = 5). The low concentration was 25 μmol·L^{-1}, and the high concentration was 50 μmol·L^{-1}. (Mean ± SD, $^{**}P < 0.01$, $^{***}P < 0.001$ *vs* DMSO group; $^{***}P < 0.001$ *vs* control group; $^{\#}P < 0.05$, $^{\#\#}P < 0.01$, $^{\#\#\#}P < 0.001$ *vs* model group)

League Against Rheumatism indicate that anti-SSA/Ro antibody, foci of lymphocytic infiltration of the submandibular gland, and salivary flow serve as diagnostic markers for SS [15]. Experimental studies were conducted using the NOD/Ltj mouse model, which is widely recognized as a standard animal model for SS research [16]. AS-OD, a commonly prescribed TCM formula for SS treatment in China, demonstrates efficacy in alleviating SS symptoms and presents a potential therapeutic approach for SS management.

SS patients typically exhibit reduced salivary accumulation rates compared to healthy individuals, coupled with elevated levels of anti-SSA/Ro and anti-SSB/La antibodies [17]. AQP5, the sole protein directly associated with saliva secretion, primarily regulates salivary production and secretion [18]. Fatigue represents one of the most common SS symptoms, manifesting as decreased physical endurance, reduced activity, and mental depression [19]. This study revealed that AS-OD significantly enhanced salivary flow rate, decreased anti-SSA/Ro and anti-SSB/La antibody levels, reduced lymphocytic infiltration foci, increased AQP5 expression in submandibular glands, and alleviated fatigue, validating AS-OD's therapeutic efficacy for SS.

SS typically manifests through autoimmune epitheliitis, chronic inflammation, and Th17/Treg cell ratio imbalance. Autoimmune epitheliitis, initiated by irregular autoantigen expression in exocrine gland epithelial cells, promotes lymphocyte recruitment and amplifies inflammatory cytokine (including TNF-α, IFN-γ, IL-1β, IL-6) and chemokine production, thereby intensifying glandular inflammation and immune responses [20]. Additionally, sustained inflammation and immune responses lead to Th17 cell overactivation, resulting in extensive lymphocyte tissue infiltration [21, 22]. Research on experimental models and patients indicates that an elevated Th17/Treg ratio significantly exacerbates SS, while its reduction ameliorates the condition [23, 24]. This investigation demonstrated that AS-OD effectively reduced TNF-α, IFN-γ, IL-1β, IL-6, IL-18, CXCL9/10 levels and modulated Th17/Treg cell balance, thus diminishing inflammation and immune responses.

The PI3K/AKT pathway serves a crucial function in autoimmune diseases by regulating cellular survival and apoptosis [13]. Irregular activation of the PI3K/AKT pathway leads to submandibular gland structural disorders and potential fibrosis [25, 26]. Furthermore, PI3K/AKT influences inflammation-induced apoptotic salivary gland epithelial cell death and Th17 differentiation in autoimmune diseases [27, 28]. AS-OD inhibited apoptosis in TNF-α and IFN-γ-stimulated A-253 cells, while PI3K/AKT agonists reversed these effects, indicating that AS-OD mitigates submandibular gland cell apoptosis through the PI3K/AKT pathway.

Growing evidence demonstrates JAK's involvement in autoimmune disease regulation [14, 29]. In SS, various cytokines activate JAK, which phosphorylates STAT and enhances inflammatory cytokine production, including CXCL9/10 [29, 30]. CXCL9/10 subsequently attracts T-cells, particularly CXCR3^{+} T cells, toward focal tissue, intensifying lymphocyte infiltration [31]. The findings revealed that AS-OD suppressed inflammatory cytokine and CXCL9/10 production through JAK1/STAT3 inhibition and prevented T cell recruitment to submandibular glands, thereby reducing glandular hyperimmunization and inflammation.

Both AS and OD represent frequently utilized herb pairs in the clinical treatment of SS within TCM practice in China. Multiple studies demonstrate that *Astragalus* and *Salvia* possess anti-inflammatory and autoimmunity properties. Total *Astragalus* flavonoids regulated Th17/Th1/Treg cell differentiation *via* JAK/STAT [32]. Research revealed that Tanshinone I suppressed the IL-6-mediated activation of the JAK/STAT3 signaling pathway [33]. Dihydrotanshinone I reduced inflammation through the regula-

tion of Th17 and inhibition of STAT1/STAT3 [34]. The AS herb pair improved dry mouth symptoms in SS by enhancing AQP5 expression [35], suggesting that AS may serve a primary function in AS-OD. Studies have also documented the anti-inflammatory and immunomodulatory effects of *Ophiopogon* and *Dendrobium*. Compound 511 derived from *Ophiopogon* improved immunosuppression by restoring the Treg/Th17 balance [36]. *Dendrobium* polysaccharide mitigated the irregular expression of AQP5 and reduced apoptosis to ameliorate SS [37]. Erianin extracted from *Dendrobium* demonstrated inhibitory effects on Th17 overactivation in collagen-induced arthritis mice [38]. These findings collectively provide scientific evidence supporting the synergistic effect of the herb pair combination in AS-OD.

5. Conclusion

This study presents the first demonstration that AS-OD enhances salivary flow rate, diminishes lymphocyte infiltration, alleviates fatigue, and modulates Th17/Treg cell balance in NOD/Ltj mice. Furthermore, AS-OD inhibits apoptosis through the PI3K/AKT pathway and regulates lymphocyte chemotaxis by decreasing CXCL9/10 production *via* the JAK1/STAT3 pathway, thereby reducing hyperimmunization, chronic inflammation, and glandular damage in SS. The combination of AS and OD herb pairs exhibited favorable outcomes both symptomatically and mechanistically, suggesting its potential as a promising therapeutic approach for SS treatment.

Funding

This work was supported by the National Natural Science Foundation of China (No. 82074341).

Availability of supporting information

Supporting information for this work can be obtained by contacting the corresponding authors *via* E-mail.

Declaration of competing interest

The authors declare that they have no conflicts of interest in this work.

References

1 Andre F, Bockle B C. Sjogren's syndrome. *J Dtsch Dermatol Ges*. 2022;20(7): 980-1002. https://doi.org/10.1111/ddg.14823.
2 Yura Y, Hamada M. Outline of salivary gland pathogenesis of Sjogren's syndrome and current therapeutic approaches. *Int J Mol Sci*. 2023;24(13): 11179. https://doi.org/10.3390/ijms241311179.
3 Ramos-Casals M, Brito-Zeron P, Bombardieri S, et al. EULAR recommendations for the management of Sjogren's syndrome with topical and systemic therapies. *Ann Rheum Dis*. 2020;79(1):3-18. https://doi.org/10.1136/annrheumdis-2019-216114.
4 Lysik D, Niemirowicz-Laskowska K, Bucki R, et al. *Artificial saliva*: challenges and future perspectives for the treatment of xerostomia. *Int J Mol Sci*. 2019; 20(13):3199. https://doi.org/10.3390/ijms20133199.
5 Basones-Martinez A, Mattila R, Gomez-Font R, et al. Immunomodulatory drugs: oral and systemic adverse effects. *Med Oral Patol Oral Cir Bucal*. 2014;19(1):e24-31. https://doi.org/10.4317/medoral.19087.
6 Li D, Guo H, Niu L, et al. Clinical value-oriented research paradigm about inheritance and innovation development of TCM dominant diseases. *Chin Herb Med*. 2023;15(4):476-84. https://doi.org/10.1016/j.chmed.2023.09.002.
7 Liu J, Zhou H, Li Y, et al. Meta-analysis of the efficacy in treatment of primary sjogren's syndrome: traditional Chinese medicine *vs* western medicine. *J Tradit Chin Med*. 2016;36(5):596-605. https://doi.org/10.1016/S0254-6272(16)30078-4.
8 Zhen W, Cao L, Du X. Progress in the compatibility mechanism of huangqi (Astragali Radix). *J Liaoning Univ Tradit Chin Med*. 2023;25(10):205-9. https://doi.org/10.13194/j.issn.1673-842x.2023.10.039.
9 Yang Y, Zhao Y, Zhang L. Analysis on the application characteristics of dendrobium in guide to clinical practice with medical records. *Jilin J Chin Med*. 2023;43(06):720-3. https://doi.org/10.13463/j.cnki.jlzyy.2023.06.023.
10 Qin Y, Lin C, Liu D, et al. Wangxinchang's experience in treating Sjogren's syndrome with method of invigorating qi, nourishing yin and removing blood stasis. *Liaoning J Tradit Chin Med*. 2018;45(02):259-61. https://doi.org/10.13192/j.issn.1000-1719.2018.02.010.
11 Ren Y, Liu D, Zhou D, et al. Effects of yiqi yangyin quyu prescription on the expression of AQP5 and M3R in submandibular glands of NOD mice with Sjogren syndrome. *TC Drug Res Clin Pharmacol*. 2023;34(05):613-91. https://doi.org/10.19378/j.issn.1003-9783.2023.05.006.
12 Karin N. CXCR3 ligands in cancer and autoimmunity, chemoattraction of effector T cells, and beyond. *Front Immunol*. 2020;11:976. https://doi.org/10.3389/fimmu.2020.00976.
13 Kapsogeorgou EK, Stergiou IE, Chatzis L, et al. The role of the AKT signaling pathway in Sjogren's syndrome. *Mediterr J Rheumatol*. 2023;34(1):113-6. https://doi.org/10.31138/mjr.34.1.113.
14 Benucci M, Bernardini P, Coccia C, et al. JAK inhibitors and autoimmune rheumatic diseases. *Autoimmun Rev*. 2023;22(4):103276. https://doi.org/10.1016/j.autrev.2023.103276.
15 Shiboski C H, Shiboski S C, Seror R, et al. 2016 American college of rheumatology/European league against rheumatism classification criteria for primary Sjogren's syndrome: a consensus and data-driven methodology involving three international patient cohorts. *Arthritis Rheumatol*. 2017; 69(1):35-45. https://doi.org/10.1002/art.39859.
16 Abughanam G, Maria O M, Tran S D. Studying Sjogren's syndrome in mice: what is the best available model? *J Oral Biol Craniofac Res*. 2021;11(2):245-55. https://doi.org/10.1016/j.jobcr.2020.12.001.
17 Kamounah S, Taybo N, Chiang S, et al. Immunoassay detects salivary anti-SSA/Ro-52 autoantibodies in seronegative patients with primary Sjogren's syndrome. *Immunohorizons*. 2023;7(7):554-61. https://doi.org/10.4049/immunohorizons.2300043.
18 Chivasso C, D'Agostino C, PARISIS D, et al. Involvement of aquaporin 5 in Sjogren's syndrome. *Autoimmun Rev*. 2023;22(3):103268. https://doi.org/10.1016/j.autrev.2023.103268.
19 Maeland E, Miyamoto ST, Hammenfors D, et al. Understanding fatigue in Sjogren's syndrome: outcome measures, biomarkers and possible interventions. *Front Immunol*. 2021;12:703079. https://doi.org/10.3389/fimmu.2021.703079.
20 Ogawa Y, Takeuchi T, Tsubota K. Autoimmune epithelitis and chronic inflammation in Sjogren's syndrome-related dry eye disease. *Int J Mol Sci*. 2021;22(21):11820. https://doi.org/10.3390/ijms222111820.
21 Wang J, Zhao X, Wan Y Y. Intricacies of TGF-beta signaling in Treg and Th17 cell biology. *Cell Mol Immunol*. 2023;20(9):1002-22. https://doi.org/10.1038/s41423-023-01036-7.
22 Knochelmann HM, Dwyer CJ, Bailey SR, et al. When worlds collide: Th17 and Treg cells in cancer and autoimmunity. *Cell Mol Immunol*. 2018;15(5):458-69. https://doi.org/10.1038/s41423-018-0004-4.
23 Fei Y, Zhang W, Lin D, et al. Clinical parameter and Th17 related to lymphocytes infiltrating degree of labial salivary gland in primary Sjogren's syndrome. *Clin Rheumatol*. 2014;33(4):523-9. https://doi.org/10.1007/s10067-013-2476-z.
24 Matsui K, Sano H. T helper 17 cells in primary Sjogren's syndrome. *J Clin Med*. 2017;6(7):65. https://doi.org/10.3390/jcm6070065.
25 Manganelli P, Fietta P. Apoptosis and Sjogren syndrome. *Semin Arthritis Rheum*. 2003;33(1):49-65. https://doi.org/10.1053/sarh.2003.50019.
26 Ren Y, Cui G, Gao Y. Research progress on inflammatory mechanism of primary Sjogren syndrome. *Zhejiang Unvi J Med Sci*. 2021;50(6):783-94. https://doi.org/10.3724/zdxbyxb-2021-0072.
27 Cai Y, Sun R, Wang R, et al. The activation of Akt/mTOR pathway by bleomycin in epithelial-to-mesenchymal transition of human submandibular gland cells: a treatment mechanism of bleomycin for mucoceles of the salivary glands. *Biomed Pharmacother*. 2017;90:109-15. https://doi.org/10.1016/j.biopha.2017.02.098.
28 Jiang CH, Xi Z, Jia W, et al. *Andrographolide sulfonate* alleviates rheumatoid arthritis by inhibiting glycolysis-mediated activation of PI3K/AKT to restrain Th17 differentiation. *Chin J Nat Med*. 2024;22(4):1-15. https://doi.org/10.1016/S1875-5364(24)60627-8.
29 Banerjee S, Biehl A, Gadina M, et al. JAK-STAT signaling as a target for inflammatory and autoimmune diseases: current and future prospects. *Drugs*. 2017;77(5):521-46. https://doi.org/10.1007/s40265-017-0701-9.
30 Li S, Fan G, Li X, et al. Modulation of type I interferon signaling by natural products in the treatment of immune-related diseases. *Chin J Nat Med*. 2023;21(1):3-18. https://doi.org/10.1016/S1875-5364(23)60381-4.
31 Zhang J, Zhang X, Shi X, et al. CXCL9, 10, 11/CXCR3 axis contributes to the progress of primary Sjogren's syndrome by activating GRK2 to promote T lymphocyte migration. *Inflammation*. 2023;46(3):1047-60. https://doi.org/10.1007/s10753-023-01791-9.
32 Han XY, Xu N, Yuan JF, et al. Total flavonoids of Astragalus inhibit activated $CD4^+T$ cells and regulate differentiation of Th17/Th1/Treg cells in experimental autoimmune encephalomyelitis mice by JAK/STAT and NFκB signaling pathways. *Am J Chin Med*. 2023;51(5):1233-48. https://doi.org/10.1142/S0192415X23500568.
33 Wang W, Li J, Ding Z, et al. Tanshinone I inhibits the growth and metastasis of osteosarcoma *via* suppressing JAK/STAT3 signalling pathway. *J Cell Mol Med*. 2019;23(9):6454-65. https://doi.org/10.1111/jcmm.14539.
34 Zhang Y, Li C, Li S, et al. Dihydrotanshinone I alleviates crystalline silica-induced pulmonary inflammation by regulation of the Th immune response and inhibition of STAT1/STAT3. *Mediators Inflamm*. 2019;2019:3427053. https://doi.org/10.1155/2019/3427053.
35 Lin Q, Zhang Q. Effects of *Astragalus membranaceus* and *Salvia miltiorrhiza* on the expression of aquaporin-5 in submandibular glands of rat with Sjogren's syndrome. *Stomatology*. 2010;30(08):473-6. https://doi.org/10.13591/j.cnki.kqyx.2010.08.002.
36 Li Z, Sun Q, Liu Q, et al. Compound 511 ameliorates MRSA-induced lung injury by attenuating morphine-induced immunosuppression in mice *via* PI3K/AKT/mTOR pathway. *Phytomedicine*. 2023;108: 154475. https://doi.org/10.1016/j.phymed.2022.154475.
37 Lin X, Shaw PC, Sze SC, et al. Dendrobium officinale polysaccharides ameliorate the abnormality of aquaporin 5, pro-inflammatory cytokines and inhibit apoptosis in the experimental Sjogren's syndrome mice. *Int Immunopharmacol*. 2011;11(12):2025-32. https://doi.org/10.1016/j.intimp.2011.08.014.
38 Tsai SW, Wang JH, Chang YK, et al. Erianin alleviates collagen-induced arthritis in mice by inhibiting Th17 cell differentiation. *Open Life Sci*. 2023;18 (1):20220703. https://doi.org/10.1515/biol-2022-0703.